JOURNAL OF COMPUTATIONAL PHYSICS 43, 315–326 (1981)

A Numerical Algorithm for Remote Sensing of Thermal Conductivity

Y. M. CHEN

Department of Applied Mathematics and Statistics, State University of New York, Stony Brook, New York 11794

AND

J. Q. LIU

Department of Applied Mathematics, Harbin Institute of Technology, Harbin, People's Republic of China

Received January 29, 1981

The applicability of the new iterative numerical algorithm of the pulse-spectrum technique (PST) to solve the inverse problem in remote sensing of the thermal conductivity of a nonhomogeneous material is demonstrated for the one-dimensional case. Numerical simulations are carried out to test the feasibility and to study the general characteristics of this technique without the real measurement data. It is found that PST does give excellent results and is more robust in solving the inverse problem of the diffusion equation than that of the wave equation. Various possible extensions of PST for solving a more general class of inverse problems of diffusion equations are pointed out.

INTRODUCTION

Thermal conductivity of a nonhomogeneous material can be inferred numerically from a small number of experimental data obtained through remote sensing techniques on the boundary as opposed to *in situ* techniques in the interior. From the experimentalist's point of view, for the ease of performing a reliable experiment, the measured physical quantity should be as fundamental as possible; in this case, the termperature measurement is preferred to the heat flux measurement. Often this type of remote sensing problems can be formulated as ill-posed inverse problems of partial differential equations in mathematical analysis, and usually the solution of an inverse problem is not unique and does not depend continuously on the given data.

The inverse problems for linear and nonlinear diffusion equations have been studied by many researchers in the past and the present. In particular, the questions of existence and uniqueness, the numerical and the analytic methods in constructing approximate solutions have been treated by Jones [1], Douglas and Jones [2], Cannon [3, 4], and Cannon and DuChateau [5–8]. However, the techniques they

0021-9991/81/100315-12$02.00/0

employ require the knowledge of the heat flux at the boundary which cannot be easily measured. Moreover, these techniques have not been fully developed for computation and cannot be readily extended to solve three-dimensional inverse problems with complex geometry. In this paper we introduce the "pulse-spectrum technique" (PST)—an iterative computational algorithm—for determining the unknown thermal conductivity of a nonhomogeneous material from the surface measurements of the temperature and the temperature gradient (instead of heat flux). It is more suitable for numerical computation and can be readily extended to solve three-dimensional inverse problems. The basic idea of the pulse-spectrum technique is that data are measured in the time-domain with compact support (pulse-shaped functions) and the synthesis of the unknown coefficient is carried out numerically in the complex frequency-domain by an iterative algorithm.

The PST was first introduced by Tsien and Chen [9] for solving an idealized velocity inverse problem in fluid dynamics (an inverse problem for the linear wave equation); then it was further developed by Chen and Tsien [10] to have the capability of handling the noise, poorly distributed and inadequately measured data. Later it was used to solve an inverse problem in electromagnetic wave propagation by Tsien and Chen [11], and recently it has been extended successfully to solve inverse problems of a nonlinear acouctic wave equation by Hatcher and Chen [12]. Moreover, the discretized version of this iterative algorithm under idealized conditions has been proved to converge quadratically [13] which is quite efficient from the numerical computation point of view.

The main purpose of the present paper is to demonstrate the applicability of the new numerical algorithm of PST to remote sensing of the thermal conductivity of a material. For simplicity, the formulation of the inverse problem of a linear one-dimensional diffusion equation is presented, and the basic numerical algorithm is given in the next section. Then numerical simulations are carried out to test the feasibility and to study the intrinsic characteristics of this numerical algorithm without the real measurement data. Finally, in the last section a comprehensive discussion of the numerical results and their implication in the actual implementation of this computational algorithm are given; moreover, the practical ways of generalization of PST to solve cases involving simultaneous determination of several unknown coefficients, nonlinear diffusion equations, and three-dimensional problems are pointed out.

Numerical Algorithm (Pulse-Spectrum Technique)

Consider the following initial-boundary-value problem of a one-dimensional linear diffusion equation:

$$\partial/\partial x \cdot [k(x)\,\partial u/\partial x] - \rho c\,\partial u/\partial t = 0, \qquad 0 \leqslant x \leqslant 1, \quad 0 \leqslant t < \infty,$$
$$u(x, 0) = 0, \qquad u(0, t) = f(t), \qquad u(1, t) = g(t), \tag{1}$$

and

$$\partial u/\partial x|_{x=0} = h(t),$$

where $u(x, t)$ is the temperature, $k(x)$ is the thermal conductivity, ρ is the constant density and c is the constant specific heat. Here the inverse problem is to determine $k(x)$ from known ρ and c and measured $f(t)$, $g(t)$ and $h(t)$, functions of t with compact supports (or pulses) and Laplace transformable.

The pulse-spectrum technique (PST) calls for the Laplace transformation of the above linear system (1) so that the entire system is transformed from time-domain to the complex frequency-domains; then the corresponding system is

$$\begin{gathered} \partial/\partial x \cdot [k(x)\, \partial v(x, s)/\partial x] - s\rho c v(x, s) = 0, \qquad 0 \leqslant x \leqslant 1, \\ v(0, s) = \mathbf{f}(s), \qquad v(1, s) = \mathbf{g}(s), \end{gathered} \tag{2}$$

and

$$\partial v(0, s)/\partial x = \mathbf{h}(s).$$

Now the inverse problem is to determine $k(x)$ from ρ, c, $\mathbf{f}(s)$, $\mathbf{g}(s)$ and $\mathbf{h}(s)$.

The iterative numerical algorithm begins by letting

$$v_{n+1} = v_n + \delta v_n, \quad k_{n+1} = k_n + \delta k_n, \qquad n = 0, 1, 2, 3, \ldots, \tag{3}$$

where $k_0(x)$ is the initial guess of the unknown coefficient $k(x)$, $|k_n| > |\delta k_n|$ and $|v_n| > |\delta v_n|$, and $\delta k_n(0) = \delta k_n(1) = 0$. Upon substituting (3) into (2), neglecting terms of $O\{(\delta v_n)^2\}$, $O\{(\delta k_n)^2\}$ and higher, and assuming that $\partial^2 k_n/\partial x^2$ and higher-order derivatives are small, one obtains a system for v_n

$$\partial/\partial x \cdot [k_n(x)\, \partial v_n/\partial x] - s\rho c v_n = 0, \qquad 0 \leqslant x \leqslant 1,$$

$$v_n(0, s) = \mathbf{f}(s) \qquad \text{and} \qquad v_n(1, s) = \mathbf{g}(s)$$

and a system for δv_n

$$\begin{gathered} \partial/\partial x \cdot [k_n(x) \partial \delta v_n/\partial x] - s\rho c\, \delta v_n = -\delta k_n \partial^2 v_n/\partial x^2 - (\partial \delta k_n/\partial x)(\partial v_n/\partial x), \\ \delta v_n(0, s) = \delta v_n(1, s) = 0. \end{gathered} \tag{5}$$

By using the method of Green's function, the differential equation (5) can be change to a Fredholm integral equation of the first kind which relates $\delta k_n(x)$ to $\delta v_n(x, s)$:

$$\int_0^1 G_n(x, x', s) \cdot \partial/\partial x' \cdot [\delta k_n(x')\, \partial v_n/\partial x']\, dx' = -\delta v_n(x, s), \tag{6}$$

or

$$\int_0^1 \partial G_n(x, x', s)/\partial x \cdot \partial/\partial x' \cdot [\delta k_n(x')\, \partial v_n/\partial x']\, dx' = -\partial \delta v_n(x, s)/\partial x, \tag{7}$$

where $G_n(x, x', s)$ is the Green's function of the differential operator in (5) and it can be computed numerically in general.

For the purpose of accelerating the rate of convergence, the right hand side of (7) can be replaced by $\partial v_n(x, s)/\partial x - \partial v(x, s)/\partial x$. After setting $x = 0$ and a simple integration by parts, one obtains the following Fredholm integral equation of the first kind for $\delta k_n(x)$:

$$\int_0^1 \partial^2 G_n(0, x', s)/\partial x\, \partial x' \cdot \partial v_n(x', s)/\partial x' \cdot \delta k_n(x')\, dx' = \mathbf{h}(s) - \partial v_n(0, s)/\partial x, \tag{8}$$

whereas the same procedure applied to (6) will only lead to the trivial identity, zero equal to zero. Moreover, for the one-dimensional case here the derivative of Green's function in (8) can be derived exactly as

$$\begin{aligned} G_n(x, x', s) &= -M_n(x, s)\, N_n(x', s), \qquad 0 < x < x', \\ &= -M_n(x', s)\, N_n(x, s), \qquad x' < x < 1, \end{aligned}$$

where $M_n(x, s)$ and $N_n(x, s)$ are two linearly independent solutions of the homogeneous form of (5) and satisfy the boundary conditions,

$$\begin{gathered} M_n(0, s) = 0, \qquad dM_n(0, s)/dx = k_n^{-1}(0)\, \mathbf{f}^{-1}(s), \\ N_n(0, s) = \mathbf{f}(s), \qquad N_n(1, s) = 0. \end{gathered}$$

Hence $\partial G_n(0, x', s)/\partial x = -k_n^{-1}(0)\, \mathbf{f}^{-1}(s)\, N_n(x', s) = -k_n^{-1}(0)\, \mathbf{f}^{-1}(s)\, \hat{v}_n(x', s)$, where $\hat{v}_n(x, s)$ is the part of $v_n(x, s)$ satisfying (4) with $\mathbf{g}(s) = 0$. For the purpose of computational efficiency, Eq. (8) can be further reduced to

$$\int_0^1 [\partial v_n(x', s)/\partial x'\,][\partial \hat{v}_n(x', s)/\partial x']\, \delta k_n(x')\, dx' = k_n(0)\, \mathbf{f}(s)[\partial v_n(0, s)/\partial x - \mathbf{h}(s)]. \tag{9}$$

Equations (3), (4) and (9) form the basic structure for each iteration in the iterative numerical algorithm of PST. First, a numerical integration subroutine is used to evaluate the Laplace transforms $\mathbf{f}(s)$, $\mathbf{g}(s)$ and $\mathbf{h}(s)$ at $s = s_i$, $i = 1, 2, 3, \ldots, I$. Then these discrete values will be used to solve Eqs. (4) and (9) numerically. The two-point boundary-value problem (4) can be solved numerically by simply using the second-order finite difference method [14]. To solve the ill-posed Fredholm integral equation of the first kind (9), here we prefer to use the Tikhonov's regularization method with second-order stabilizers [15]. The essence of the first cycle of iteration is given in the following diagram and the procedure for other cycles is exactly the same:

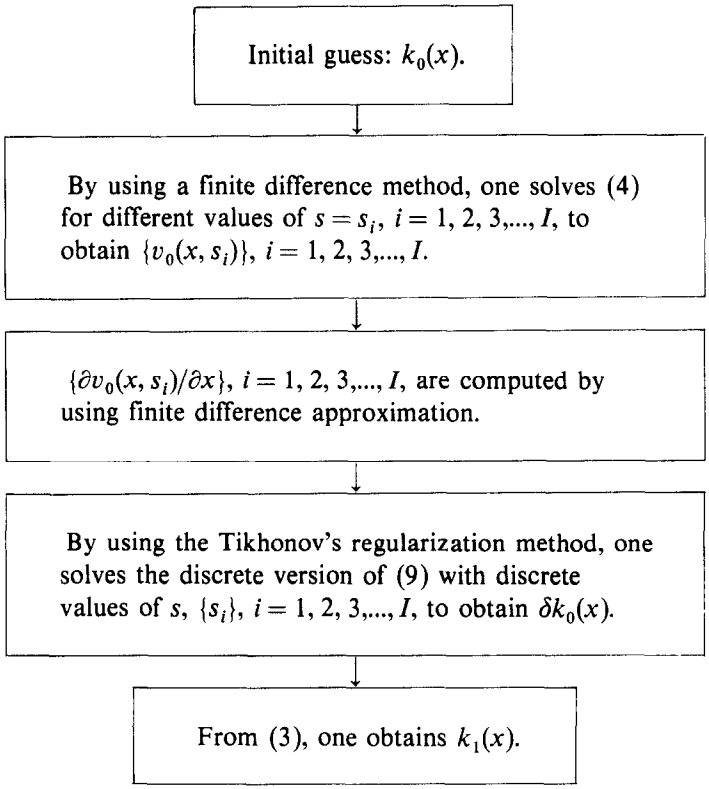

It is important to notice that each cycle of iteration consists basically of first solving the direct two-point boundary-value problem (4) I times and then solving the Fredholm integral equation of the first kind (9) once.

Numerical Simulation

In order to test the feasibility and to study the general characteristics of the new PST computational algorithm without the real measurement data, the following numerical simulation procedure is carried out:

First, one chooses a $k^*(x)$ which is supposed to represent the correct thermal conductivity of an object and also the boundary conditions $f(t)$ and $g(t)$ which are supposed to represent the measured data partially. Their Laplace transforms $\mathbf{f}(s)$ and $\mathbf{g}(s)$ are numerically computed for a chosen discrete set of $s = s_i$, $i = 1, 2, 3,..., I$. Then the two-point boundary-value problems (2) (omitting the third boundary condition) with the chosen $k^*(x)$, $\mathbf{f}(s_i)$ and $\mathbf{g}(s_i)$ are solved by using the finite difference method; thus one generates the rest of the supposedly measured data $\mathbf{h}(s_i)$, $i = 1, 2, 3,..., I$, by a simple finite difference approximation.

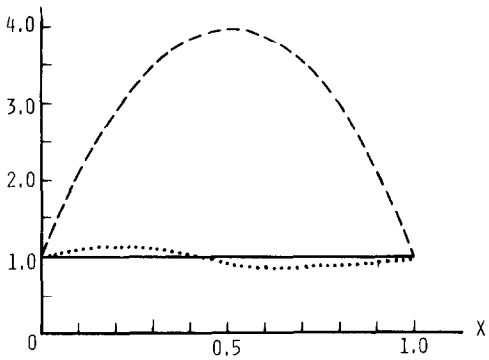

FIG. 1. Comparison of the calculated $k_5(x)$ (···) and the exact $k^*(x)$ (——), with the initial guess $k_0(x)$ (– – –).

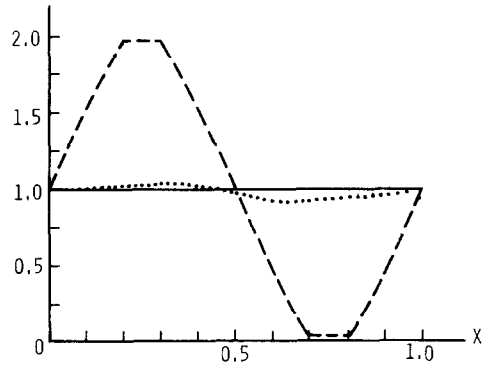

FIG. 2. Comparison of the calculated $k_7(x)$ (···) and the exact $k^*(x)$ (——), with the initial guess $k_0(x)$ (– – –).

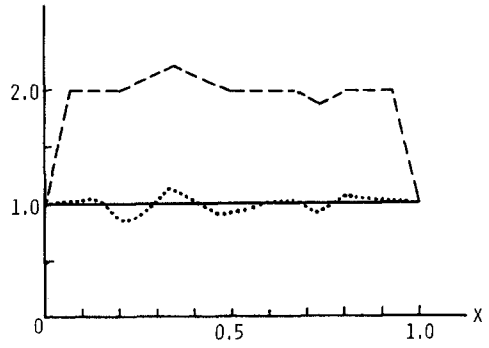

FIG. 3. Comparison of the calculated $k_{14}(x)$ (···) and the exact $k^*(x)$ (——), with the initial guess $k_0(x)$ (– – –).

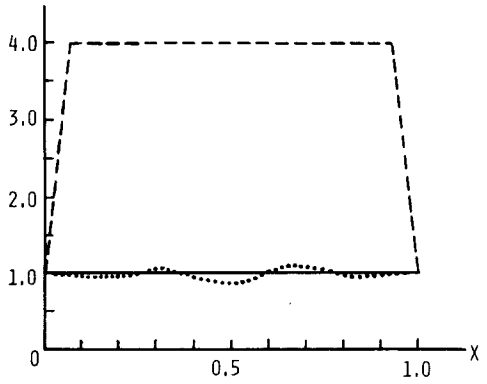

FIG. 4. Comparison of the calculated $k_{10}(x)$ (···) and the exact $k^*(x)$ (——), with the initial guess $k_0(x)$ (– – –).

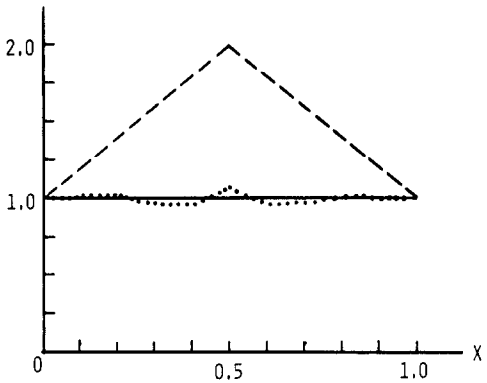

FIG. 5. Comparison of the calculated $k_{10}(x)$ (···) and the exact $k^*(x)$ (——), with the initial guess $k_0(x)$ (– – –).

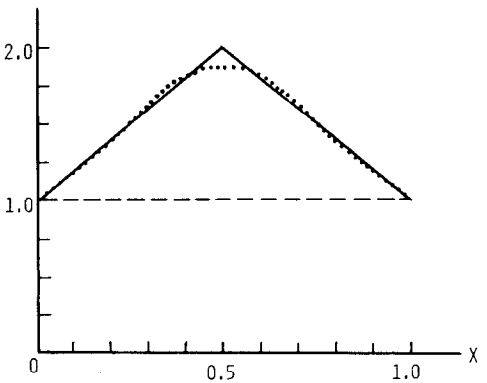

FIG. 6. Comparison of the calculated $k_{10}(x)$ (···) and the exact $k^*(x)$ (——), with the initial guess $k_0(x)$ (– – –).

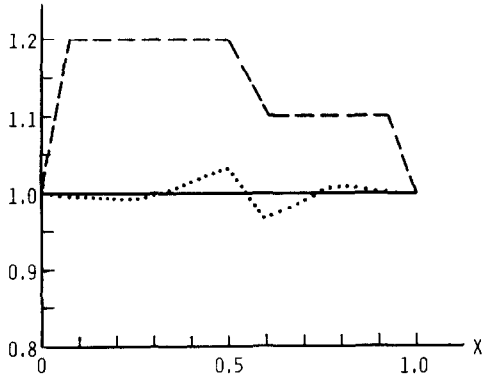

FIG. 7. Comparison of the calculated $k_{10}(x)$ (···) and the exact $k^*(x)$ (——), with the initial guess $k_0(x)$ (– – –).

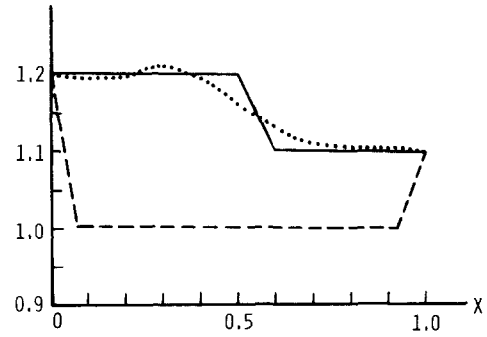

FIG. 8. Comparison of the calculated $k_{10}(x)$ (···) and the exact $k^*(x)$ (——), with the initial guess $k_0(x)$ (– – –).

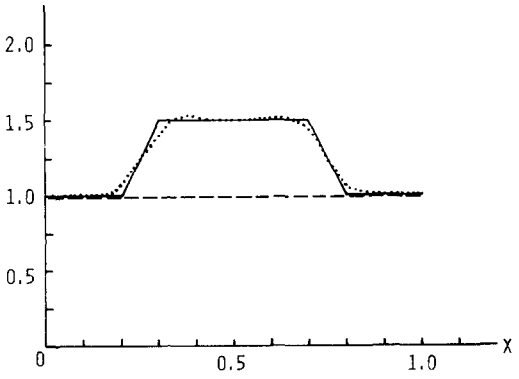

FIG. 9. Comparison of the calculated $k_{10}(x)$ (···) and the exact $k^*(x)$ (——), with the initial guess $k_0(x)$ (– – –).

TABLE I

	Fig.								
	1	2	3	4	5	6	7	8	9
I_0	6.928	2.236	3.830	9.00	1.844	1.844	0.490	0.510	1.114
I_N	0.355	0.138	0.291	0.361	0.187	0.122	0.056	0.058	0.079
N	5	7	14	10	10	10	10	10	10

Next, $k_0(x)$ is assumed. Hence upon solving (3), (4) and (9) numerically, $k_1(x)$ is obtained. Then in a similar manner $k_2(x)$ is obtained. One continues this procedure until finally a numerical limit $k_N(x)$ is reached. Other than the truncation, round-off, numerical integration and the finite difference approximation errors in both generating the numerical data and computing $k_N(x)$, any norm $\|k^*(x) - k_N(x)\|$ can be used as a criterion for evaluating the performance of the computational algorithm of PST.

The numerical simulation here is carried out for a general class of $k^*(x)$ and $k_0(x)$, e.g., constants, piecewise-linear continuous functions and oscillatory functions. In fact, the interchange of the functions for $k^*(x)$ and $k_0(x)$ results in no significant differences in $k_N(x)$'s except in some of the fine details. Hence for avoiding the expense in generating numerical data, a single $k^*(x)$ is used for most of the numerical examples here; instead, various different $k_0(x)$'s are used for each numerical example. Furthermore, for avoiding the expense in performing numerical Laplace transformation, $f(t) = H(t)$, the Heaviside unit step function, and $g(t) = 0$ are chosen such that $\mathbf{f}(s) = s^{-1}$ and $\mathbf{g}(s) = 0$. Here $s_i = i$, $i = 1, 2, 3, \ldots, 11$, are used in our computation. The trapezoidal rule is used to discretize the integrals.

The numerical results are plotted in Figs. 1 – 9. The maximum norms of $k^*(x) - k_N(x)$ and $k^*(x) - k_0(x)$ for various cases can be estimated from the graphs

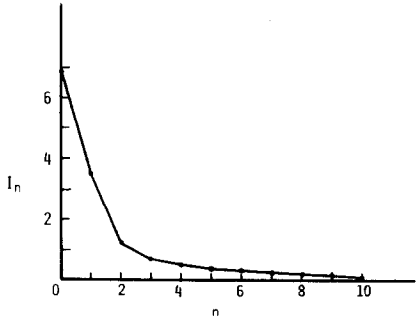

FIG. 10. I_n as a monotonic decreasing function of n shown for the numerical example in Fig. 1.

in these figures. The L_2 norms, $I_n = \|k^*(x) - k_n(x)\|_2$, $n = 0, N$, for various cases are tabulated in Table I. I_n as a function of n for the numerical example in Fig. 1 is shown in Fig. 10.

Discussion

The numerical results in Figs. 1–9 have demonstrated that the PST iterative numerical algorithm does give excellent results in inferring the thermal conductivity from a set of measured data of surface temperature and its gradient for a general class of $k^*(x)$ and $k_0(x)$. Moreover, PST is shown to be more robust in solving the inverse problem of the diffusion equation than that of the wave equation [9–11], e.g., $\text{Max.}_x |k^*(x) - k_0(x)|/\text{Max.}_x |k^*(x)|$ is much larger here than the corresponding ratio in the case of the wave equation. This outcome is not surprising at all, because one of the key steps responsible for the success of the PST iterative numerical algorithm is how well one can evaluate the Fredholm integral equation of the first kind. Here the kernel in the Fredholm integral equation of the first kind is a monotonic function while the corresponding kernel for the case of the wave equation is an oscillatory function; hence the numerical problem here is better conditioned than that of the wave equation. Although here all of the examples are solved under the assumption that $\delta k_n(0) = \delta k_n(1) = 0$, $n = 0, 1, 2, 3,...$, which means the thermal conductivity at the boundary surface is a priori known, this assumption is not entirely without real justification, for in practice the actual material property at the surface can be measured by direct means.

It is interesting to observe that except in the neighborhood of boundary all of the approximate numerical solutions $k_N(x)$'s do inherit the genetic characteristics of the initial guesses $k_0(x)$'s, e.g., if $k_0(x)$ is smooth, then $k_N(x)$ is also smooth; if $k_0(x)$ is a piecewise-linear continuous function with a corner at x', then $k_N(x)$ also has a corner at x'. This simplies that $k_N(x)$ depends on $k_0(x)$, i.e., for different $k_0(x)$'s, the PST iterative numerical algorithm will lead to slightly different $k_N(x)$'s. If the numerical algorithm is reasonable robust, then any one of the approximate solutions will be an acceptable approximation. This numerical computation phenomenon can be attributed to the accumulation of those non-negligible errors in computing each iterate. In the case here, most of these computational errors come from the regularization procedure in solving the Fredholm integral equation of the first kind. Examples and proofs are given by Surmont and Chen [16] and Chen and Surmont [17] in the case of solving the Hammerstein integral equation of the first kind by using Newton-like iterative algorithms. More abstract results can be found in [18]. In the neighborhoods of the boundary, the constraints $\delta k_n(0) = \delta k_n(1) = 0$ are strong enough to prevent the above-mentioned inheritance problem.

The accuracy of the numerical algorithm can be improved greatly if more efforts are made in computing each individual step of the numerical algorithm and if larger numbers of s_i's are used and their values are properly chosen according to either the minimum error criterion [19] or the well-conditioned matrix criterion [20] in solving

the Fredholm integral equation of the first kind. In the case of the measurement data contaminated by instrument noise or other random errors, the PST iterative numerical algorithm is still applicable except that the Backus and Gilbert linear inversion technique [21–23] will be used to solve the Fredholm integral equation of the first kind with erroneous data instead of the Tikhonov's regularization method as for the case of the wave equation [10, 11].

The PST iterative numerical algorithm can be extended to solve three-dimensional inverse problems in a straightforward manner, because the finite difference method or the finite element method is just as adaptable to solve any three-dimensional boundary-value problem with arbitrary finite domain as to solve the one-dimensional two-point boundary-value problem, and the Tikhonov's regularization method is also as adaptable to solve the three-dimensional Fredholm integral equation of the first kind as to solve the one-dimensional case. However, many practical difficulties do exist, e.g., the maximization of the computational efficiency, the minimization of the computer core storage, the selection of a minimum amount of data for maximum computational accuracy, the accurate computation of the iterative Green's function, etc.

The PST iterative numerical algorithm also can be generalized to solve the inverse problems of special classes of nonlinear diffusion equations as for the case of nonlinear wave equations [12]. Moreover, it can be further extended to the simultaneous determination of several unknown coefficients of a diffusion equation. The efforts in carrying out the above-mentioned possible generalizations and applications are either well under way or just started. The results will be reported in the near future.

REFERENCES

1. B. J. JONES, JR., *J. Math. Mech.* **11** (1962), 907–918.
2. J. DOUGLAS, JR. AND B. F. JONES, JR., *J. Math. Mech.* **11** (1962), 919–926.
3. J. R. CANNON, *Duke Math. J.* **30** (1963), 313–323.
4. J. R. CANNON, *J. Math. Anal. Appl.* **8** (1964), 188–201.
5. J. R. CANNON AND P. DUCHATEAU, *Int. J. Eng. Sci.* **11** (1973), 783–794.
6. J. R. CANNON AND P. DUCHATEAU, *SIAM J. Appl. Math.* **24** (1973), 298–314.
7. J. R. CANNON AND P. DUCHATEAU, *J. Heat Transfer* **100** (1978), 503–507.
8. J. R. CANNON AND P. DUCHATEAU, *SIAM J. Appl. Math.* **39** (1980), 272–289.
9. D. S. TSIEN AND Y. M. CHEN, *in* "Computational Methods in Nonlinear Mechanics" (Proceedings, Int. Conf. Computational Methods in Nonlinear Mechanics, The University of Texas at Austin), pp. 935–943, 1974.
10. Y. M. CHEN AND D. S. TSIEN, *J. Comput. Phys.* **25** (1977), 366–385.
11. D. S. TSIEN AND Y. M. CHEN, *Radio Sci.* **13** (1978), 775–783.
12. R. P. HATCHER AND Y. M. CHEN, in preparation.
13. Y. M. CHEN, *in* "Proceedings, International Symp. Ill-Posed Problems: Theory and Practice, University of Delaware, Newark, October 1979."
14. H. B. Keller, "Numerical Methods for Two-Point Boundary-Value Problems," Ginn (Blaisdell), Waltham, Mass., 1968.
15. A. N. TIKHONOV AND V. Y. ARSENIN, "Solutions of Ill-Posed Problems," Wiley, New York, 1977.

16. J. SURMONT AND Y. M. CHEN, *J. Comput. Phys.* **13** (1973), 288–302.
17. Y. M. CHEN AND J. SURMONT, *Appl. Math. Comput.* **2** (1976), 197–228.
18. W. C. RHEINBOLDT, *SIAM J. Numer. Anal.* **5** (1968), 42–63.
19. E. TSIMIS, "On the Inverse Problem by Means of the Integral Equation of the First Kind," Ph.D. thesis, Department of Applied Mathematics & Statistics, State University of New York at Stony Brook, 1977.
20. F. HAGIN, *J. Comput. Phys.* **36** (1980), 154–169.
21. G. BACKUS AND F. GILBERT, *Geophys. J. Astron. Soc.* **13** (1967), 247–276.
22. G. BACKUS AND F. GILBERT, *Geophys. J. R. Astron. Soc.* **16** (1968), 169–205.
23. G. BACKUS AND F. GILBERT, *Philos. Trans. R. Soc. London Ser. A* **266** (1970), 123–192.